The SSCM: an adaptation of Cameron's target decomposition to actual calibration SAR requirements

R. Touzi and F. Charbonneau*
Canada Centre for Remote Sensing
Natural Resources Canada
588 Booth Street, Ottawa
Ontario, Canada K1A OY7

Abstract— **Cameron's coherent target decomposition (CTD) and classification are discussed in the context of SAR, and the limitations of Cameron's classification are examined. It is shown that Cameron's classification leads to a coarse scattering segmentation because of the large class dispersion that corresponds to a SAR system with about ± 5 dB channel imbalance. The application of Cameron's method within known SAR radiometric calibration requirements limits the utility of the classification. A new method, named the symmetric scattering characterization method (SSCM), is introduced to better exploit the information provided by the largest target symmetric scattering component, under coherent conditions. The SSCM, which expressed the symmetric scattering in term of the Poincaré sphere angles, permits a better characterization of target symmetric scattering and the generation of coherent scattering segmentation of much higher resolution, in comparison with Cameron's coarse segmentation.**

I. Introduction

An interesting classification method, which is based on coherent target decomposition (CTD), was introduced in [1]. Cameron's classification extracts, in each illuminated resolution cell, the largest symmetric scattering component from the total radar return, and assigns it to one of six symmetric elemental scatterer classes: the trihedral, diplane, dipole, cylinder, narrow diplane, and quarter wave device [1]. This method has been widely used for the characterization and identification of point targets such as ships [7], [8] and small planes. In Section II, Cameron's CTD and classification are discussed in the context of SAR, and the limitations of Cameron's classification are examined. Cameron's CTD is then reconsidered in Section III, to develop a new method, named the SSCM method, that exploits better the information provided by Cameron's CTD in the context of coherent scattering. The new method is validated for ocean scattering characterization and ship identification using Convair-580 polarimetric SAR data collected off shore Cape Race, Newfoundland, Canada.

* under contract with TGIS Consultant

II. Analysis of Cameron's Coherent Target Decomposition and classification

A. Cameron's CTD

Inspired by the work of Huynen [4], Cameron associates importance to a class of targets termed symmetric. A symmetric target as defined in [4] is a target having an axis of symmetry in the plane orthogonal to the radar line of sight direction (LOS). Symmetric targets have a scattering matrix which can be diagonalized by a rigid rotation about the LOS in a basis of linear eigen polarizations. Huynen introduced a technique for CTD in terms of target parameters that are orientation invariant, and particularly in terms of the polarization configurations that maximizes the received power in [4]. The ellipticity angle τ_m of the maximum polarization determines the symmetric-nonsymmetric nature of the scattering; $\tau_m = 0$ for symmetric scattering and $\tau_m \neq 0$ for asymmetrical scattering.

Cameron developed an algorithm that maximizes the symmetrical component of coherent scattering [1]. Under target and SAR system reciprocity assumption, the scattering matrix is expressed in terms of the Pauli matrices, as: $[S] = \alpha[S_a] + \beta[S_b] + \gamma[S_c]$. Scattering is symmetric if there exists an angle of rotation ψ_a that cancels the projection of $[S]$ on the non symmetric Pauli direction $\vec{S}_c$, where $\vec{S}_c$ is the vectorial form of the Pauli matrix $[S_c]$. This leads to the following expression for the symmetric part, $\vec{S}_{sym}$, as a function of the angle $\theta = -2\psi_a$ [1]:

$$\vec{S}_{sym} = \alpha\vec{S}_a + \epsilon \cdot [\cos\theta \cdot \vec{S}_b + \sin\theta \cdot \vec{S}_c] \tag{1}$$

The symmetric component $\vec{S}_{sym}$ of the total scattering $\vec{S}$ (the vectorial form of $[S]$), reaches its maximum for the angle θ that satisfies the following relationship, for $\beta \neq \gamma$ [1]:

$$\tan(2\theta) = \frac{\beta\gamma^* + \beta^*\gamma}{|\beta|^2 - |\gamma|^2} \tag{2}$$

After diagonalization, the largest symmetric component $\vec{S}_{sym}^{max}$ can be expressed in the trihedral-dihedral basis, ($\vec{S}_a$, $\vec{S}_b$), as:

$$\vec{S}_{sym}^{max} = \alpha\vec{S}_a + \epsilon\vec{S}_b \tag{3}$$

where ϵ is given:

$$\epsilon = \beta \cos\theta + \gamma \sin\theta \tag{4}$$

The total scattering vector $\vec{S}$ can be expressed as the sum of two components under the following form [1]:

$$\vec{S} = A \cdot \left[\cos\tau \cdot \vec{S}_{sym}^{max} + \sin\tau \cdot [\vec{S}_{sym}^{max}]^c\right] \tag{5}$$

where $\vec{S}_{sym}^{max}$ is the largest symmetric component, $[\vec{S}_{sym}^{max}]^c$ is the remaining component, and the degree to which $\vec{S}$ deviates from $\vec{S}_{sym}^{max}$ is measured by the angle τ [1]:

$$\cos\tau = \frac{\|(\vec{S}, \vec{S}_{sym}^{max})\|}{\|\vec{S}\|\|\vec{S}_{sym}^{max}\|} \tag{6}$$

The term $\cos\tau$, which also corresponds to the ratio of the largest symmetrical component intensity, $|\alpha|^2 + |\epsilon|^2$, to the total intensity, $|\alpha|^2 + |\beta|^2 + |\gamma|^2$, will be referred to as the degree of symmetry, d_{sym}.

B. Cameron's classification: Analysis and discussion

B.1 Symmetric scatter classification metric

Cameron introduced a classification method for operational use of his CTD [1]. If the scatterer is assigned to symmetric scattering class, the largest symmetric scattering component is derived, and the scatterer is assigned to the closest elemental scatterer class of trihedral, dihedral, dipole, cylinder, narrow diplane, and quarter wave device. These reference point targets are presented as diamonds in Figure 1, and the complex disk is segmented into patches that corresponds to the 6 classes of elemental scatterers. A metric distance $d(z, z_{ref})$, defined in [1] as a function of the scatterer parameter z and the reference elemental scatterer parameter z_{ref}, is used to assign each image pixel to the closest elemental scatterer class.

B.2 Application to SAR data

A polarimetric data set collected with Environment Canada's airborne Convair-580 SAR, off Cape Race (Newfoundland, Canada) in 2000 [3], is used for this study. The data set covers an open ocean area with a ship imaged at 43° incidence angle. Figure 2 presents Cameron's classification of the maximized symmetric scattering. Pixels that do not correspond to symmetric scattering are not classified. As seen from Figure 2, most of the sea pixels are assigned to the cylinder class, whereas most of ship pixels are assigned to the narrow dihedral and dipole classes. From these results, one tends to conclude that sea clutter is dominated by cylinder scattering, whereas ship scattering is dominated by dipole and narrow dihedral scatterers, as in [7], [8].

B.3 Problems with Cameron's classification

For each pixel, the classification metric distance d to the various reference elemental scatterers is calculated to assign the pixel to the closest elemental scatterer class. Cameron mentions that such a method leads to "coarse" segmentation. In fact, this method tolerates a radiometric dispersion of up to ±5 dB from the elemental scatterer parameter z_{ref}, as shown in Figure 1. Such a large dispersion cannot be tolerated in the context of SAR since the radiometric calibration requirements of satellite SARs are within a maximum of 0.5 dB [6].

In order to account for this gap, a radiometric decision threshold is introduced in the classification. The classification obtained with a radiometric threshold of 0.5 dB is very poor. Figure 3 presents the classification results obtained with a threshold of 1.5 dB. As seen in Figure 3, the classification obtained is of very limited interest; only few ocean pixels are assigned to the cylinder class and most of the ship pixels are unclassified. In fact, the number of classified pixels with 1.5 dB tolerance is insignificant when compared to the original classification of Figure 2.

It is apparent that Cameron's classification is misleading, and application of the method within known SAR radiometric calibration requirements significantly reduces its effectiveness. In the next section, Cameron's CTD is reconsidered in order to develop a new method, the symmetric scattering characterization method (SSCM), which better exploits Cameron's CTD.

III. Reconsideration of Cameron's CTD; The SSCM Method

A. Characterization of the maximized symmetric scattering component

The maximized symmetric component of equation (3) can be characterized by the two complex entities α and ϵ, which represent the distribution of the largest symmetric scattering component in the basis of the orthogonal vectors $\vec{S}_a$ and $\vec{S}_b$. The information provided by these two parameters can be exploited in various ways. They can be used to represent the symmetric scattering on the Poincaré sphere, as shown in the following.

B. Poincaré sphere for representation of symmetric scattering

Cameron shows that the unit disc complex representation might introduce a distortion, and he suggests instead using a closed surface that is represented in Figure 1 [1]. The Poincaré sphere inspires a more suitable representation of the maximized symmetric scattering vector expressed under equation (3) in the $(\vec{S}_a, \vec{S}_b)$ basis. After normalization by the total intensity $(|\alpha|^2 + |\epsilon|^2)$, each diagonalized symmetric scattering vector $\vec{\Lambda}_n$ can be expressed as:

$$\vec{\Lambda}_n = \begin{pmatrix} 1 & \cos(2\chi_c)\cos(2\psi_c) & \cos(2\chi_c)\sin(2\psi_c) & \sin(2\chi_c) \end{pmatrix}$$

where the Poincaré sphere angles ψ_c and χ_c can be derived from equation (3) of scattering decomposition. Each symmetric scatterer can then be represented as a point on the Poincaré unit sphere surface of latitude $2\chi_c$ and longitude $2\chi_c$, as seen in Figure 4. The quarter waves devices $\vec{\Lambda}_n(j)$

and $\vec{\Lambda}_n(-j)$ are on the North and South poles. The normalized scattering vectors of the trihedral $\vec{S}_a$, diplane $\vec{S}_b$, dipole $\vec{S}_l$, cylinder $\vec{S}_{cy}$, and narrow diplane $\vec{S}_{nd}$ are on the Equator.

In order to remove the rotation phase ambiguity, only half of the sphere is used with a ψ_c varying within the interval of $[0, \pi/2]$. If ψ_c is lying in the interval $]\pi/2, \pi]$, symmetric scattering sphere coordinates (ψ_c,χ_c) are replaced with ($\pi - \psi_c$,-χ_c), and the rotation angle ψ_a is replaced with $\psi_a \pm \pi/2$.

Only coherent symmetric scatterers can be represented as a point on the surface of the Poincaré sphere. A partially coherent symmetric scatterer is represented as a point inside the sphere at a distance from the sphere center determined by the degree of coherence of the scatterer components α and ϵ on the basis ($\vec{S}_a$, $\vec{S}_b$) given by:

$$p_{sym} = \frac{\sqrt{(<|\alpha|^2 - |\epsilon|^2>)^2 + 4.|<\alpha.\epsilon^*>|^2}}{<|\alpha|^2 + |\epsilon|^2>} \qquad (7)$$

When the symmetrical scattering is dominated by the trihedral $\epsilon = 0$ or the dihederal $\alpha = 0$, p_{sym}, which indicates the degree of coherence of the symmetrical scattering is close to 1, as should be expected. This expectation motivates our choice for this parameter p_{sym}, called degree of symmetric scattering coherence, to measure channel coherence.

IV. The SSCM method

A. SSCM schema

For an optimum exploitation of Cameron's CTD, we suggest the application of the following steps:
1. Calculation of the parameters α and ϵ of the maximum symmetric component, using Cameron's algorithm [1]
2. Classification of distributed target scattering into coherent and noncoherent classes using the p_{sym} map.
3. Classification of point target scattering into coherent and noncoherent classes using the Rican threshold.
4. Computation and analysis of the S_{max} Poincaré sphere parameters within the coherent class.

V. Examples of SSCM Applications using polarimetric Convair-580 SAR data

A. The SSCM for a high resolution characterization of ocean scattering

The SSCM is applied on the Cape Race scene of Figure 2 to generate the Poincaré sphere angles ψ_c and χ_c maps of the maximized coherent symmetric scattering S^{max}_{sym}. About 66% of the ocean coherent symmetric scattering is ($\psi_c = -16.8° \pm 17°, \chi_c = 10.8° \pm 10°$, as presented Figure 5. This angle interval was presented with 2 colours in Cameron's classification of Figure 2 that correspond to the patches called cylinder and trihedral in the disc presentation of Figure 1. Such coarse classification is misleading when we see from Figure 5 that a "pure" cylinder scattering of ($\psi_c = 18.44°, \chi_c = 0$)) represents less than 1% of the total population.

B. The SSCM for ship identification

A polarimetric data set collected with Environment Canada's airborne Convair-580 SAR [5], off Cape Race (Newfoundland, Canada) in 2000 [3], [2], was used for this study. The data set covers an open ocean area which includes a ship of 60 feet size, referenced to as the Arctic Pride (AP) and presented in Figure 6. AP was imaged with an orientation of -21° from the azimith, on the 28^{th} of March, and the 30^{th} of March 2000. On the 28^{th} of March, AP was imaged at 44° incidence angle, in calm wind conditions (7 kt at the acquisition time). On the 30^{th} of March, AP was imaged at 37° incidence angle in rough wind conditions (20 kt at the acquisition time). The antenna in the middle of the ship and the metallic feature at the back of the ship, referenced to as MID and DB in Figure 6, are potential targets of symmetric scattering. Table 1 presents the coordinates (ψ_c, χ_c) on the Poincare sphere of theses features. They correspond to a signal to clutter ratio of about 20 dB, which results in a dispersion in phase of ±5°, according to the Rice distribution. The (MID) antenna coodinates appear stable within the 2 flights with an average scattering of about (48°,3°), which is very close to a pure dipole scattering, as seen in Figure 4. The rotation angle ψ_a can then be used to estimate the pitch angle, which is also given in Table 1.

TABLE 1: Poincaré sphere coordinates (ψ_c, χ_c) in degrees of 2 mains features DB and MID.

Date	inc. ang.	Wind speed	DB	MID	Pitch
28 Mar.	44°	7 kt	(48.9°,-8.7°)	(50.9°,5.8°)	-2.7°
30 Mar.	37°	7 kt	(36°,12.2°)	(45°,0.9°)	9.6°

VI. Conclusion

Cameron's ideas about the maximization of the symmetric scattering component of target scattering is not well exploited with the coarse classification method he introduced. The large radiometric dispersion tolerated in each elemental scatterer class, and the application of the CTD decomposition method in areas of non-coherent scattering may lead to erroneous result interpretation with high resolution SARs. Adaptation of Cameron's method to the known SAR radiometric calibration requirements limits the utility of the classification.

The SSCM method introduced in this paper better exploits the information provided by the symmetric scattering component of the target return, and leads to much higher resolution characterization of target scattering, in comparison with Cameron's coarse and misleading segmentation. The SSCM looks very promizing for ship and manmade target identification. Further experimental studies are currently being conducted for an improved understanding of the physical meaning of the parameters derived with the SSCM in relationship with ocean, forest, agriculture, and point target properties. Application of the SSCM forremoval of Faraday rotation from satellite L-band polarimetric SAR data, is currently being investigated.

Acknowdlegments

The authors would like to thank the Defence Research Establishment of Ottawa for having financed a part of the data acquisition campaigns, and Dr. R.K. Hawkins from CCRS for having organized the campaigns. The support of Environment Canada which operates the system is also acknowledged.

References

[1] W.L. Cameron, N. Youssef, and L.K. Leung. Simulated polarimetric signatures of primitive geometrical shapes. *IEEE Trans. Geoscience Rem. Sens.*, 34(3):793–803, 1996.

[2] R.K. Hawkins, K.P. Murnaghan, M. Yeremy, and M. Rey. Ship detection using airborne polarimetric SAR. In *CEOS SAR Workshop Proc., Tokyo*, April 2001.

[3] R.K. Hawkins, W. Wong, and K. Murnaghan. Crusade Experiment March 2000. In *Canada Centre for Remote Sensing CCRS-TN-2000-07*, March, 2000.

[4] J.R. Huynen. Measurement of the target scattering matrix . *Proc. IEEE*, 53(8):936–946, 1965.

[5] C. E. Livingstone, A. L. Gray, R. K. Hawkins, P. W. Vachon, T. I. Lukowski, and M. LaLonde. The CCRS airborne SAR systems: Radar for remote sensing research. *Can. J. Rem. Sens.*, 21(4):468–491, 1995.

[6] P.J. Meadows, B. Rosich, and D.E. Fernandez. The performance of the ERS-2 Synthetic Aperture Radar. In *Proc. of the ERS-ENVISAT Symposium, Goteborg , Sweden*, October, 2000.

[7] R. Ringrose and N. Harris. Ship detection using polarimetric SAR data. In *Proc. of the CEOS SAR workshop, ESA SP-450, http://www.estec.esa.nl/CONFANNOUN/99b02*, October 1999.

[8] M. Yeremy, J.W.M. Campbell, K.Mattar, and T. Potter. Ocean surveillance with polarimetric SAR. *Can. J. Rem. Sens.*, 27(4):328–344, 2001.

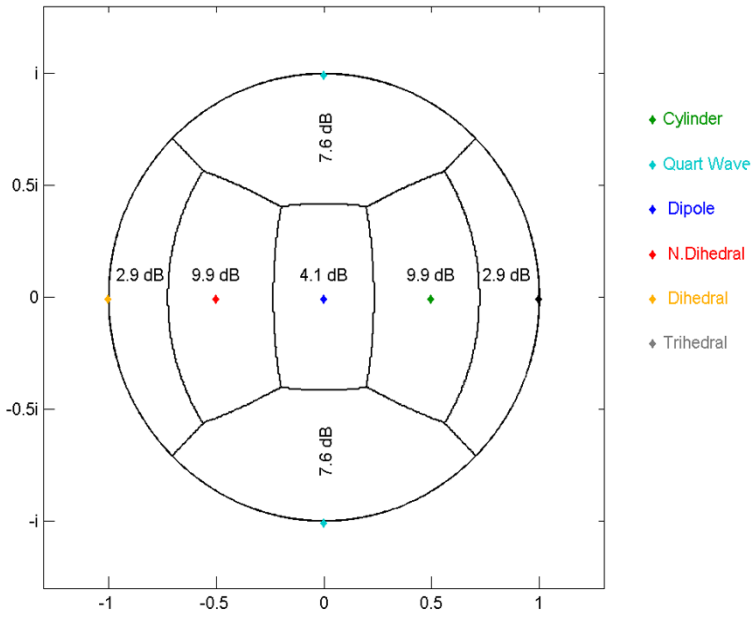

Fig. 1. *Cameron classification dispersion in the complex disc*

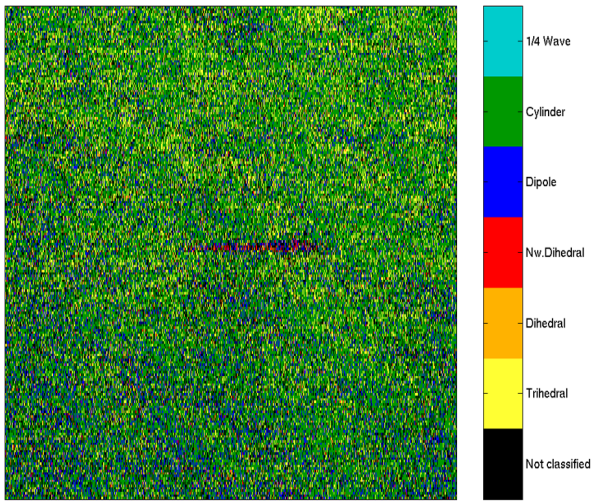

Fig. 2. *Cameron Classification*

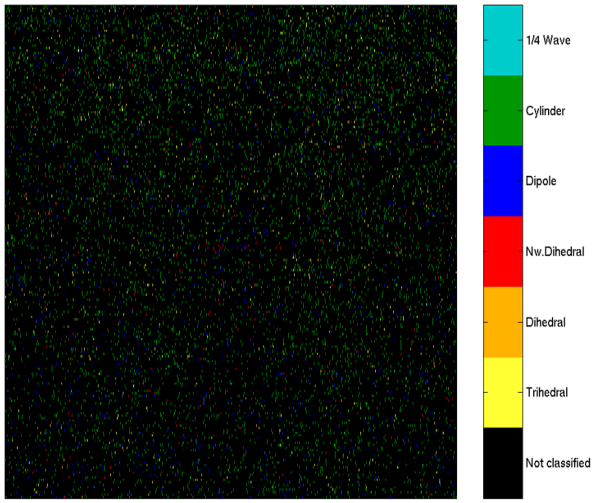

Fig. 3. *Cameron classification with 1.5 dB dispersion*

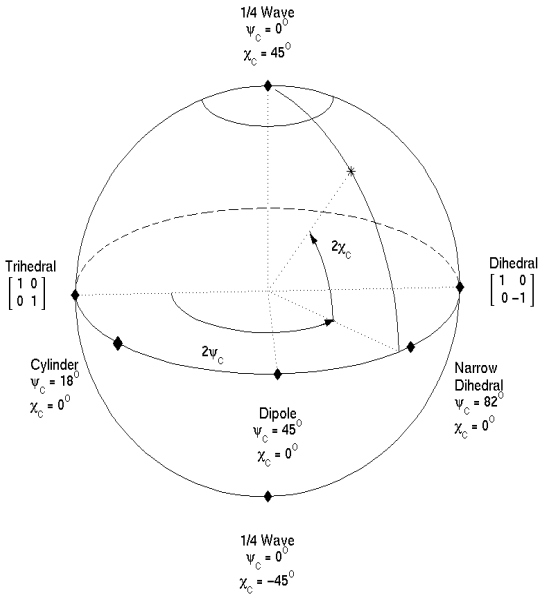

Fig. 4. S_{sym}^{max} *Target Sphere*

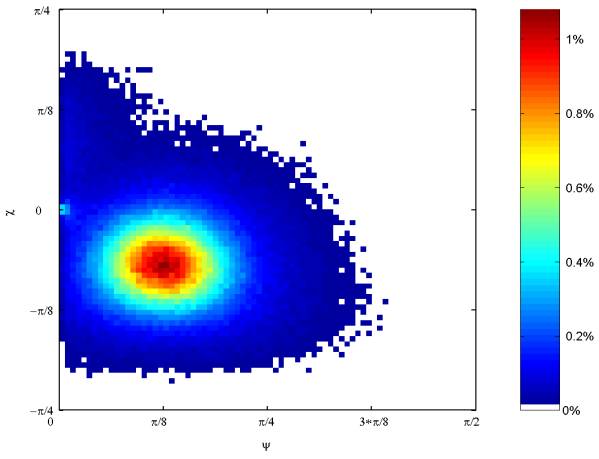

Fig. 5. *Ocean symmetric scattering in the* (ψ_c, χ_c) *plan*

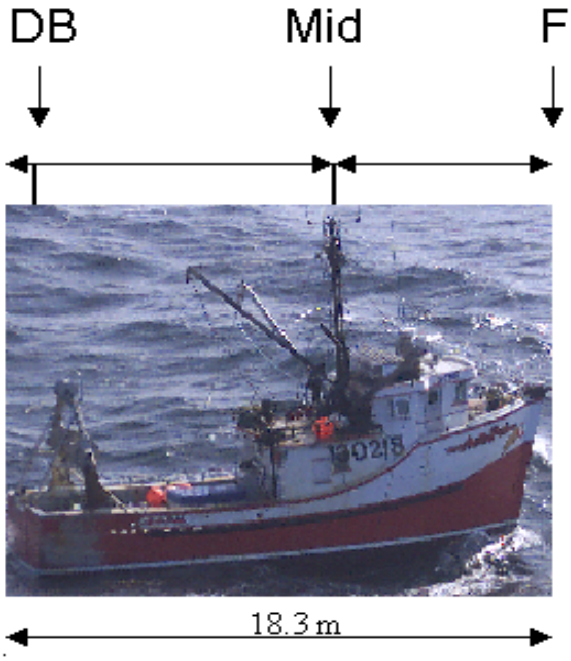

Fig. 6. *Arctic Pride (AP)*